

COMPUTATIONAL ANALYSIS OF BLAST INDUCED DAMAGE ON
NEURONS IN BRAIN DURING TRAUMATIC BRAIN INJURY.

by

DIVYA SWAMY BANDARU

Presented to the Faculty of the Graduate School of
The University of Texas at Arlington in Partial Fulfillment
of the Requirements
for the Degree of

MASTER OF SCIENCE IN.....

THE UNIVERSITY OF TEXAS AT ARLINGTON

APRIL 2016

Copyright © by Divya Bandaru 2016

All Rights Reserved



ACKNOWLEDGEMENTS

I would first like to thank my advisor Dr. Ashfaq Adnan for his incredible support and guidance. I thank Dr. Chan and Dr. Kent Lawrence for serving on my defense committee.

It would not be possible for me to achieve my career and academic goals without the unconditional love and support of my parents Mr. Suryanarayana Swamy and Mrs. Vasanthi Chepuru. Also, I would like to give many thanks to the guiding spirit of my elder sister Sowjanya Bandaru. She is just an incredible and my best friend. It is impossible to not acknowledge my fiancé Jai Parivesh Natami, who is my confidant. His affection and support are unwavering.

I would like to thank all my friends and other members of my family who have always cared and support me. I would take this opportunity to dedicate this to my father to whom I owe my career and all my achievements. With his ever so admirable wisdom guides me in every aspect of my life.

ABSTRACT

COMPUTATIONAL ANALYSIS OF BLAST INDUCED DAMAGE ON NEURONS IN BRAIN DURING TRAUMATIC BRAIN INJURY.

Divya Swamy Bandaru, MS

The University of Texas at Arlington, 2016

Supervising Professor: Dr. Ashfaq Adnan

Concussions are the most common kind of brain injuries, they are also called as mild Traumatic Brain Injuries (mTBI). In recent times, mTBIs are perceived as one of the major health problems faced by millions across the world. TBIs occur when there is a sudden acceleration or deceleration force is applied on the human brain that is encapsulated in the skull.

When blasts caused by typical IEDs (induced by explosives) in wars propagate through the head, cavitation bubbles are formed in the brain tissue. When these bubbles collapse, they form cavitation-induced shock wave. It has been found that the strains caused by cavitation-induced shock wave are much larger than the strain caused by blasts alone. In previous studies, the effect of cavitation induced shock wave on is studied on the strain rate behavior of brain tissue. In this study, cavitation induced damage is studied on axons of

neurons is studied computationally.

TABLE OF CONTENTS

ACKNOWLEDGEMENTS	iii
ABSTRACT.....	iv
LIST OF ILLUSTRATIONS.....	vii
LIST OF TABLES	ix
CHAPTER 1 INTRODUCTION	1
CHAPTER 2 SHOCK-WAVES	3
CHAPTER 3 CAVITATION.....	5
CHAPTER 4 HUMAN BRAIN.....	6
CHAPTER 5 EFFECTS OF BLASTS ON HUMAN BRAIN	12
CHAPTER 6 EFFECT OF CAVITATION BUBBLE COLLAPSE ON AXON.....	19
CHAPTER 7 CONCLUSIONS AND RESULTS.	25
REFERENCES	34
BIOGRAPHICAL INFORMATION.....	38

LIST OF ILLUSTRATIONS

Figure 1 Components of blast pressure waves [2]	4
Figure 2 Neuron parts labelled.....	7
Figure 3 Neuron with oligodendrocyte and myelin sheath.....	8
Figure 4 Illustration of evolution of varicose swelling affecting long regions of axon in brain trauma. [11].....	10
Figure 5 Evolution of axon bulbs and disconnection during trauma.	11
Figure 6 Sequence of images showing the Dynamic behavior of a single bubble in response to a simulated blast wave. [5]	14
Figure 7 Shows a pressure profile of over and under pressure blast wave phases. $t=0$ is the start of the experiment. [5]	15
Figure 8 shows the cavitation of single bubble near a ballistic edge. (a) Shows the incident blast wave direction travelling right to left. (b) Bubble initiation (circled), (c) and (d) growth, (f) collapse, and the effect on an adjacent gel slice (f to i). A local shock wave following bubble collapse resulted in highly localized hydrogel deformation (red arrows). $P_o \text{ max}=2800 \text{ kPa}$ and $P_u \text{ min}=-380 \text{ kPa}$. [5].....	16
Figure 9 Radial strain vs time plot during bubble collapse. [5].....	18
Figure 10 Plot of radial displacement vs time	20
Figure 11 Plot of radial stress vs time.....	21
Figure 12 In this figure, the points of reference for table 1 data is marked.....	22
Figure 13 Axon cross section showing tau protein and microtubules.	24

Figure 14 Scaled Tau protein elongation vs Half-length of microtubule. 25

Figure 15 MT axial strain vs half-length of microtubule..... 26

LIST OF TABLES

Table 2 Values of radial strain, radial force, and the radial stress at different points on the radial strain vs time plot.....	23
--	----

CHAPTER 1 INTRODUCTION

In recent days, the interest in Traumatic Brain Injury has risen to high levels because of its widespread presence in military soldiers and in contact sports. There are 1.7 million cases in US alone each year [13]. The peculiar behavior of biomechanical nature of TBI leads to Diffuse Axonal Injury (DAI) in the white matter of the brain. In the past these injuries were neglected by considering and just a concussion but in recent studies showed that overt axonal pathology may be present in mTBI[25].

Human head when exposed to a blast wave experience concussions, also called as mild Traumatic Brain Injury (mTBI). TBIs mainly occur because of head rotational acceleration or deceleration when the impact is induced. This rapid acceleration deforms the brain. The axon cells in the brain fail because of shear stresses. The axons present in the white matter of the brain are more prone to this failure caused by dynamic loading. This kind of failure in axons is called Diffuse Axonal Injury (DAI). It is one the main causes for mTBI or concussions. The axons are viscoelastic materials. Most of the times the axons do not fail immediately after are hit by a blast. They can even degrade after 10 years of injury.

Cavitation induced shock wave occurs when a head is

exposed to a blast. The strains caused by cavitation are much larger than just the simulated blast alone. In previous studies, the effect of cavitation induced shock wave is studied on the strain rate behavior of the soft tissue of brain. In this study cavitation induced damage on axons is studied computationally.

CHAPTER 2 SHOCK-WAVES

In wars, the blasts are caused by a various number of explosives like mortar shells, rocket propelled grenades and IEDs (Improvised explosive device , induced by an explosive blasts). In Iraq and Afghanistan, IEDs have been the most common cause for blast injuries, estimated around 40% of coalition deaths in Iraq [1, 2].

The IED have diverse designs, they typically are made by coupling an explosive charge to a detonator. IEDs incorporate shrapnel generating materials like nails, ball bearings, scrap metal, etc.

When a bomb detonates, it's solid or liquid explosive is directly converted into gas, creating a pulse of increased air pressure lasting milliseconds. The gasses rapidly expand as a sphere from the point source, forming a high pressure wave, known as blast over pressure wave (fig.1) [1, 2]. This over pressure wave travels at Mach >1 (greater than speed of sound) and it is preceded by blast wind generated by the mass displacement of air caused by the expansion of gases. This is followed by pressure drops down to near vacuum, (relatively) called as under pressure wave. This causes a momentary reversal of air flow or the blast wind is reversed. The below picture is a graph of the components of blast pressure wave.

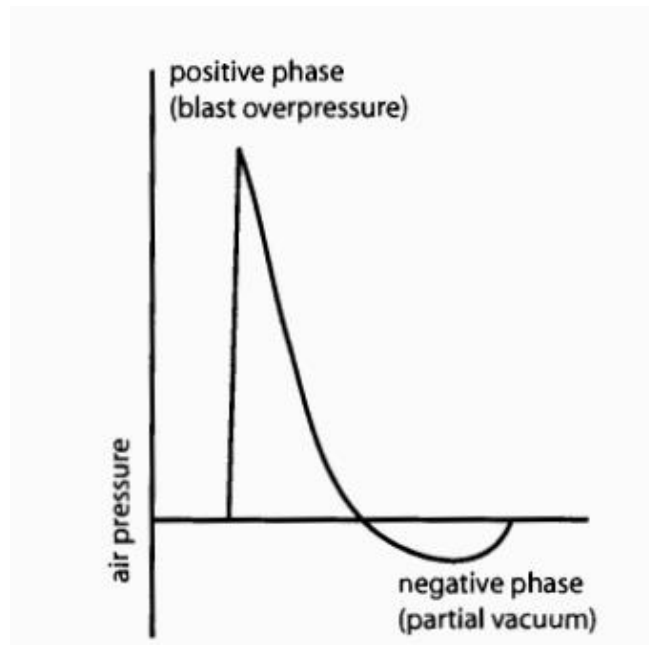


Figure 1 Components of blast pressure waves [2]

The under pressure wave is then followed by a positive pressure wave, and after that the atmosphere pressure comes down to normal.

CHAPTER 3 CAVITATION

The term cavitation is used to describe the bubble formation and its peculiar activity inside a liquid. The factors like sudden drop in pressures below the vapor pressure of the liquid aid the formation of cavitation bubbles. Some of the examples of cavitation that we can see in day to day life are boiling water in kettle, cavitation bubbles in our blood when we rise suddenly to the surface from scuba diving. We use the term cavitation to usually describe the bubble formation under very violent conditions like rupture of liquid. The cavitation bubbles are usually very harmful to the boundaries around them.

In mechanical engineering, cavitation is undesired in components like propeller shafts of boats. When propellers rotate at high speeds, and when they are designed poorly, cavitation bubbles are formed on the leading trail of the propellers. This reduces the efficiency, causes erosion and rotational speed of the propellers so this is highly unwanted in their design.

The research on cavitation in biological systems will help facilitate the application in medicine and biology. Like for example, better understanding of cavitation is helpful in gene therapy, drug delivery approaches and in the case of ballistic injuries.

CHAPTER 4 HUMAN BRAIN

Brain is the prime organ of our central nervous system. It is encased in skull, which is the bony structure that forms the human head and the skull protects the brain from injuries. The brain is the highest organ of nervous system, it receives the stimuli form sense organs.

Brain is composed of neurons, blood vessels and glial cells. Roughly there are around 86 billion neurons in an adult brain. Neuron is a basic cell of our nervous system. The main function of neuron is to transmit information through electrical as well as chemical signals. These signals are called nerve impulses.

Axon is an extended part of neural cell. It can up to a few 100 micrometers long. Its main function is to send impulses from its neuron cell body to another. Axon is a viscoelastic material, so it can withstand a substantial amount of stretch in normal day to day activities [14].

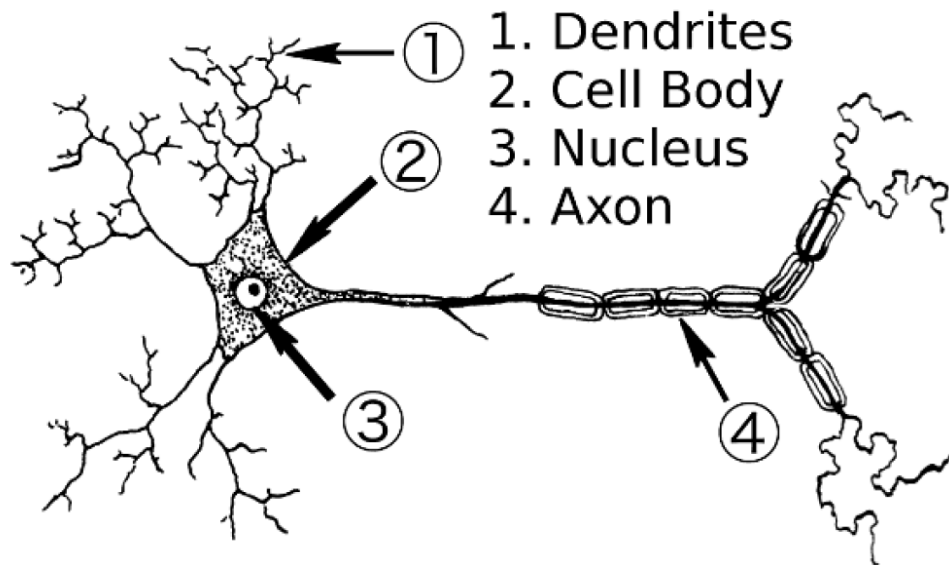


Figure 2 Neuron parts labelled.

Axon is protected by a myelin sheath; it insulates the axon fibers by wrapping the axon. This sheath helps in faster transmission of impulse signals. The axon also has its typical cytoskeletal elements that are critical for its functionality.

Mature neurons consist of three main filament structures- microtubules, microfilaments, and neuro filaments. Microtubules are about 25nm in diameter. They are hollow cylinders with 13 micro-filaments made of dimmers of alpha and beta tubulins.

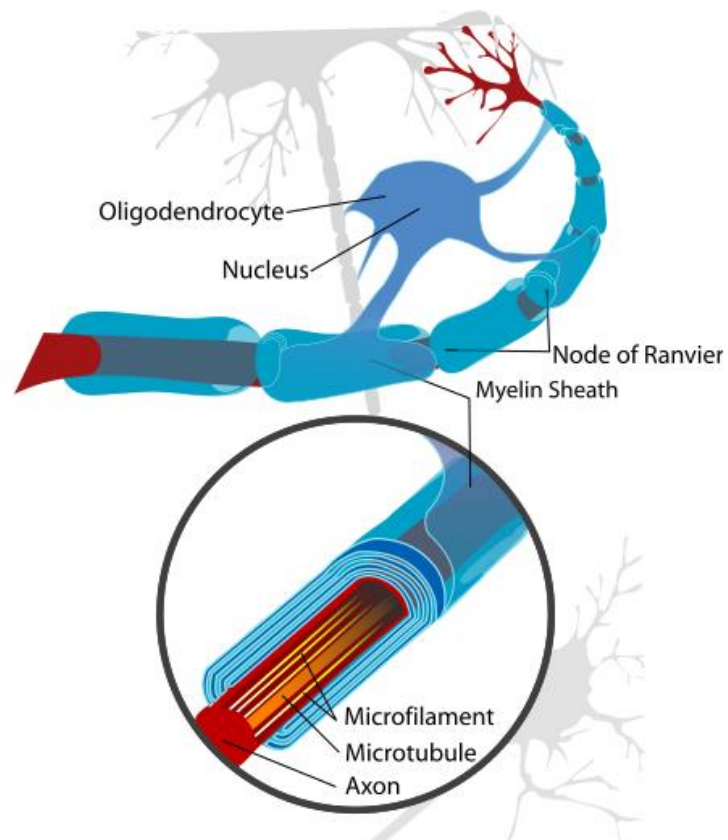


Figure 3 Neuron with oligodendrocyte and myelin sheath

Axons are ductile, that is they retain their original shape when the load is removed. But when loads are dynamic or applied very rapidly, they tend to exhibit somewhat brittle behavior. When dynamic load above the critical limit of axons is applied, they fail after a certain period of time. They can start to fail in hours or even years after the load is applied. The viscoelastic behavior of the axons in dynamic loading is very critical in TBIs. [15]

The axons swell along its length, this is known axonal varicose. When they are stretched rapidly, the axonal cytoskeleton becomes

damaged. This results in loss of elasticity and transport of axoplasmic material is impaired. [11] The transport material gets accumulated in a one place and hence the axonal varicose is formed. Calcium entry into impaired axon causes further damage and dysfunction. Ultimately the swollen axons get disconnected and contribute to changes in neuropathological changes.

Future advancements in prevention and treatment of axonal injuries is dependent on understanding the various stages of axonal injury causes and its biomechanics.

In figure below, Douglas H. Smith, et.al, 2000, show the various stages of varicose swelling evolution due to mechanical stretching of a long axon. The damage might lead to degeneration or repair of pathway. The repair mechanisms can sometimes restore the original shape and diameter of the axon pathway. The figure shows that the degeneration can occur in multiple places in an axon.[11]

In figure the evolution of axonal bulbs is demonstrated in one location. Because of localized damage in axon in one place, the swelling causes cytoskeletal disarray. The part of the axon which is away from the bulb is disconnected and in the end the entire axon degenerates.

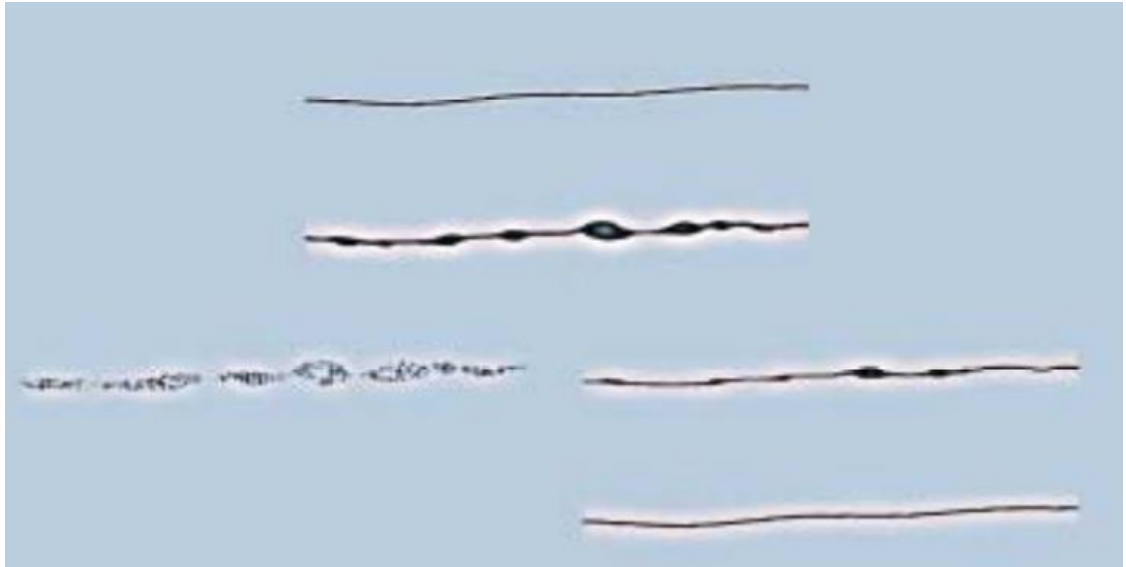


Figure 4 Illustration of evolution of varicose swelling affecting long regions of axon in brain trauma. [11]

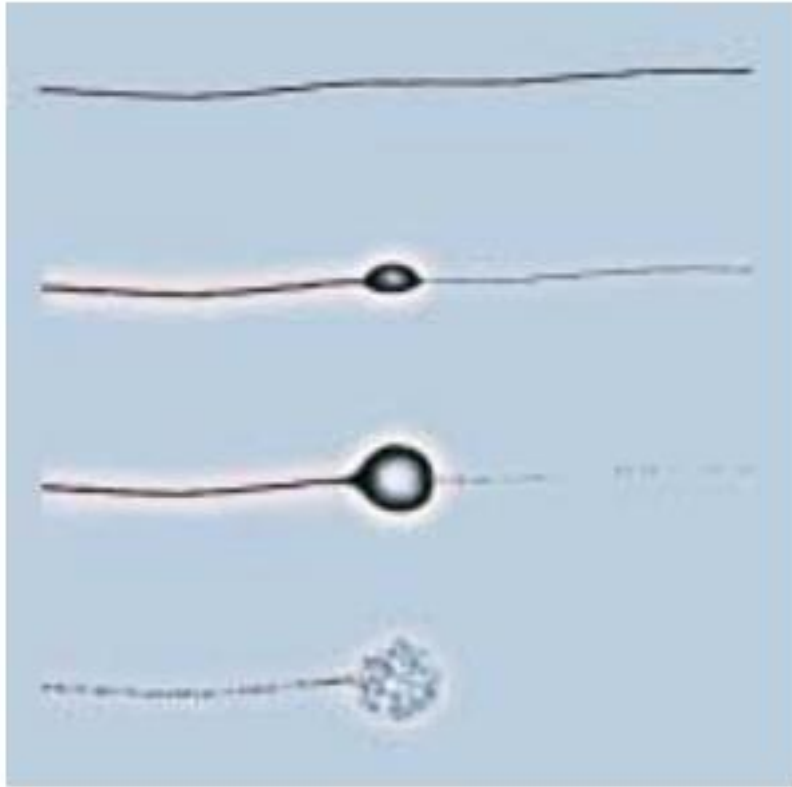


Figure 5 Evolution of axon bulbs and disconnection during trauma.

CHAPTER 5 EFFECTS OF BLASTS ON HUMAN BRAIN

The complete effect of a blast wave on the brain is not completely understood as on today. The initial mechanisms of brain injury are known to be vague. There are many possible ways that the brain can deform. They include ways like Diffuse axonal injury due to rapid accelerating – decelerating forces, skull deformation with elastic flexure, multiple wave reflections, impedance mismatch between heterogeneous tissue types, and cavitation, have been proposed[4].

In the brain, with shock loading cavitation occurs. This is due to the fact that the shock waves propagate through air as a series of over and under pressure waves. When these waves propagate through the cerebrospinal fluid which is at constant temperature (CSF) and brain tissue of the head, cavitation is formed. This phenomenon occurs because of under pressure part of blast wave, the pressure of CSF falls below its saturated vapor pressure. Cavitation bubble forms, grows and collapses in the short interval of time when the blast wave passes through the head.

Nucleation of these cavitation bubbles can either be originated between the liquid and solid boundaries of the brain tissues. Studies have also shown that the tiny air bubbles in the biological tissues also act as source for nucleation. [6].

As mentioned earlier, the strain rates are far higher in brain tissues when we consider the effects of cavitation than just the blast loads.

Y. Hong, et.al 2015, have done experiments on single seed bubble and captured the effects its collapse in hydrogel. [5] Figure 2 shows the evolution of a simulated typical cavitation bubble in a tissue surrogate. Figure 3 shows a graph of blast over and under pressure.

The time taken for this experiment was around 270 to 350 μ s. The bubble was compressed during over pressure stage (a to c) and it grows in the under pressure stage (d to h). The bubble collapses in (n) and there is some secondary growth in (o) followed by secondary collapse in (p to r). The bubble is almost spherical throughout the test. The gas seed bubble had an initial diameter < 50 μ m. [5]

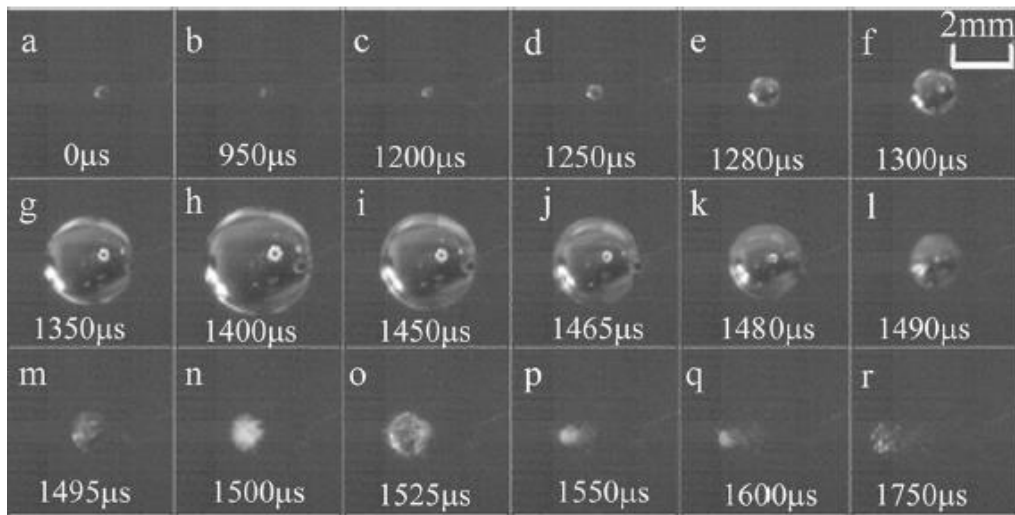


Figure 6 Sequence of images showing the Dynamic behavior of a single bubble in response to a simulated blast wave. [5]

To show the evidence of shock wave generation with bubble collapse, Y. Hong et.al. [5] Have conducted experiments were conducted on hydrogels submerged in fluids, tested in both gassed and degassed chambers. The bubble was inflated by air at calculated pressures to mimic the actual the cavitation using air guns. Figure 4 shows that the bubble collapses with local shock wave formation at high pressures.

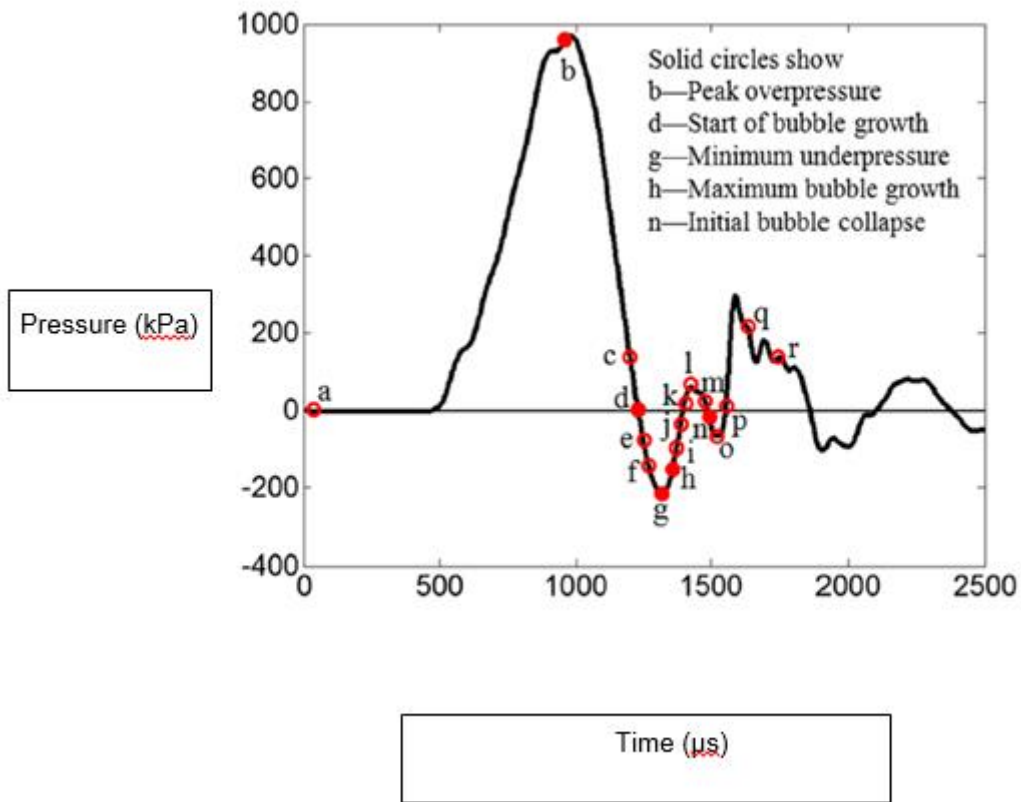


Figure 7 Shows a pressure profile of over and under pressure blast wave phases. $t=0$ is the start of the experiment. [5]

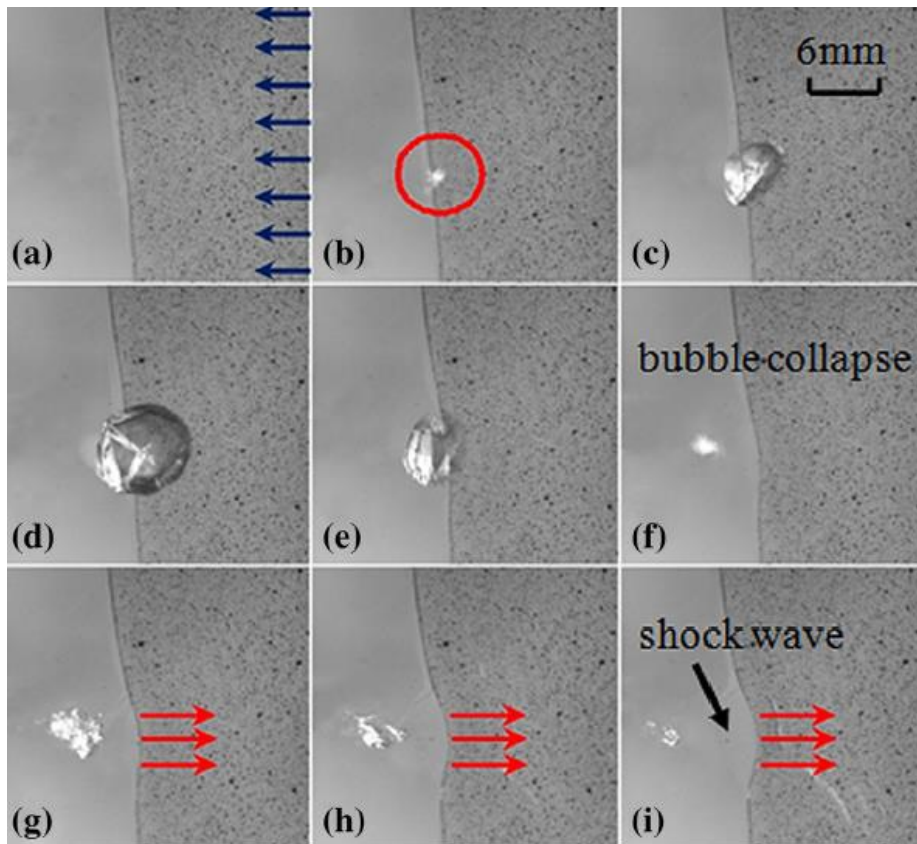


Figure 8 shows the cavitation of single bubble near a ballistic edge. (a) Shows the incident blast wave direction travelling right to left. (b) Bubble initiation (circled), (c) and (d) growth, (f) collapse, and the effect on an adjacent gel slice (f to i). A

local shock wave following bubble collapse resulted in highly localized hydrogel deformation (red arrows). $P_o \text{ max}=2800 \text{ kPa}$ and $P_u \text{ min}=-380 \text{ kPa}$. [5]

During the bubble growth, the bubble edge has compressive radial strains and the circumferential strains are observed at the bubble edge are tensile. The radial strain in hydrogel during bubble growth due to inertia are plotted in figure 9. To measure the strains, the point closest to the seed bubble not covered by growing bubble was selected.

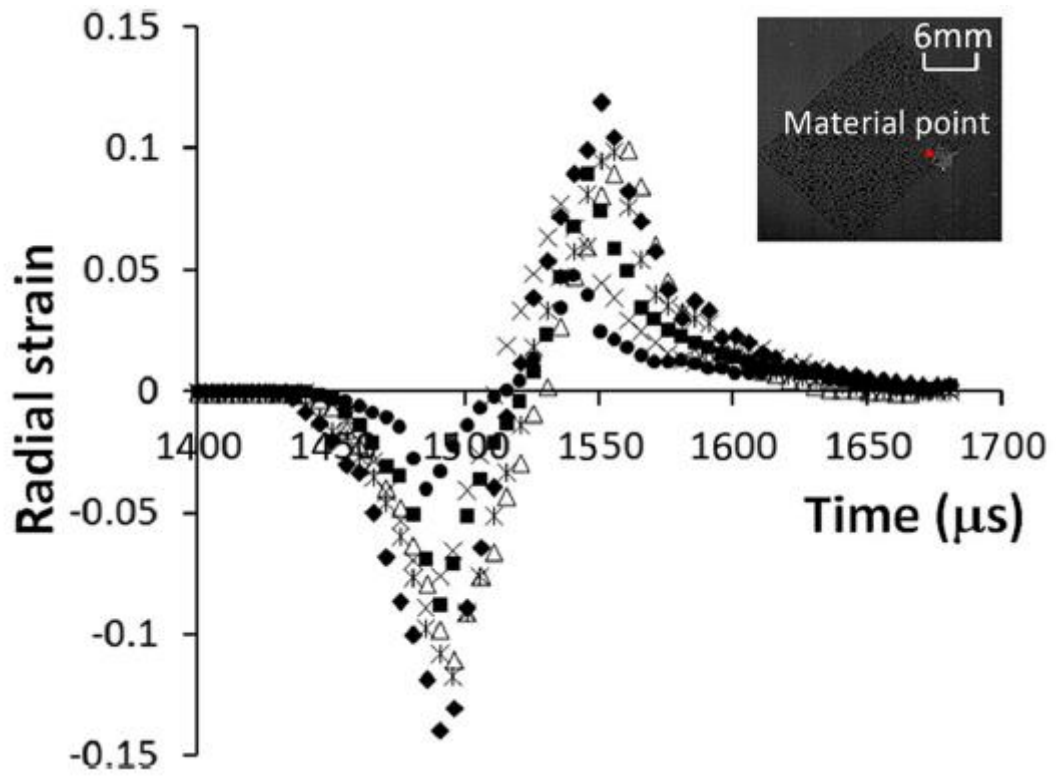


Figure 9 Radial strain vs time plot during bubble collapse. [5]

CHAPTER 6 EFFECT OF CAVITATION BUBBLE COLLAPSE ON AXON.

The experiment that has been mentioned above imitates the blast wave profile in an intracranial fluid. The soft tissue surrogate, hydrogel mimics the brain tissue. The high and low profile blast wave from this experiment when compared to experiments done on dead animal tissues (in vivo) were within relevant ranges. [5]

When a blast wave hits the brain tissue, cavitation bubbles are formed in the CSF because of presence of air pockets or on the solid-liquid boundary as discussed earlier. The effect of bubble collapse is on axon is studied in this research. Data points in Figure 9 can be used to represent the radial strain on the brain tissue. These data points represent $\epsilon_{rr}(t)$

From these data points, radial displacement is calculated by the following relation as shown in Figure 10.

$$V(t) = \epsilon_{rr}(t) * \text{radius of axon.}$$

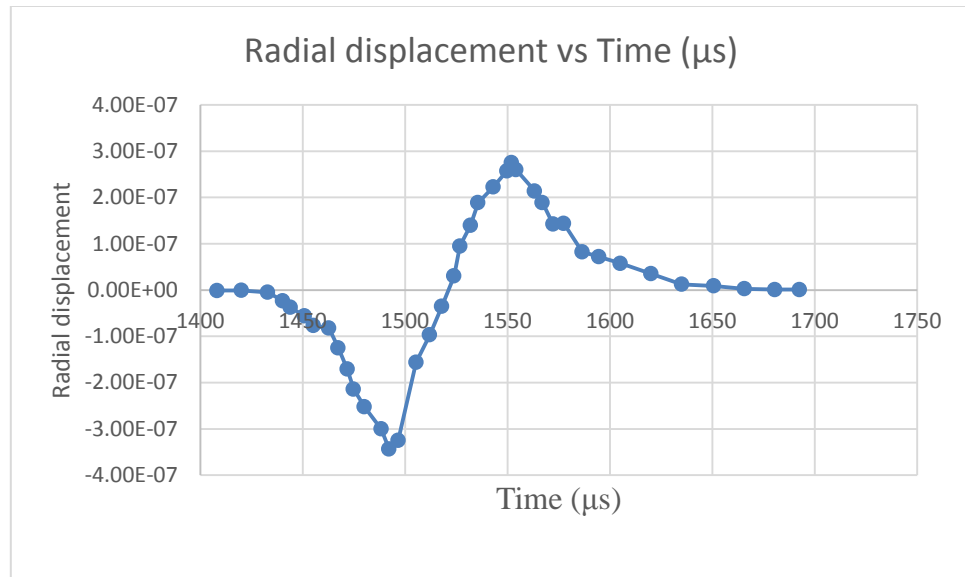


Figure 10 Plot of radial displacement vs time

We know that, $V_{max}(t) = \frac{PL}{AE}$

Where, V_{max} is the displacement, P is the force causing the radial displacement, A is the area of cross section of axon, E is the stiffness of axon. This force is used to calculate the radial stress as a function of time. This is plotted as shown in figure 11.

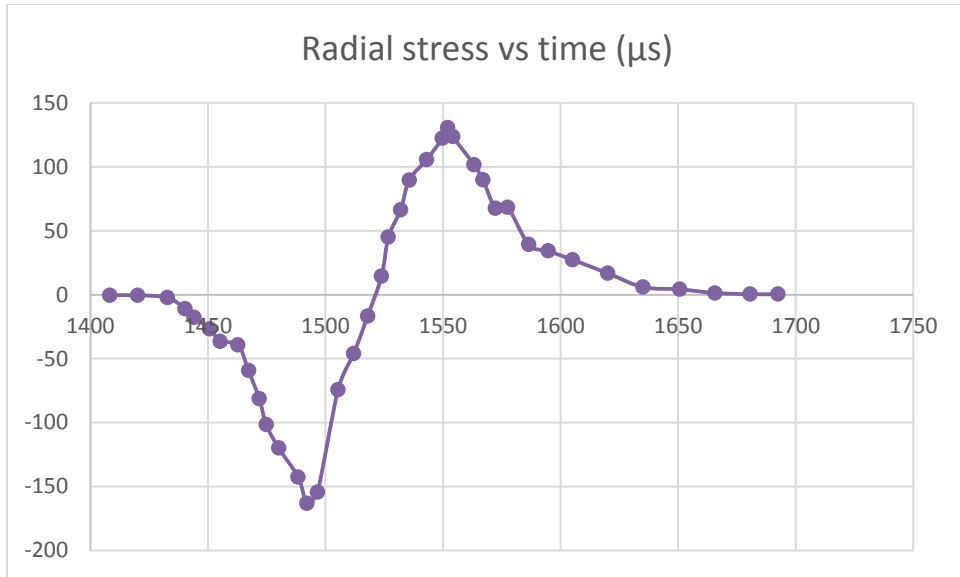


Figure 11 Plot of radial stress vs time

Now, to radial stress distribution profile on the axon due to bubble collapse as a function of time the following steps were taken. Using the below data points on the curve, we get the values for radial stress on axon and on a microtubule.

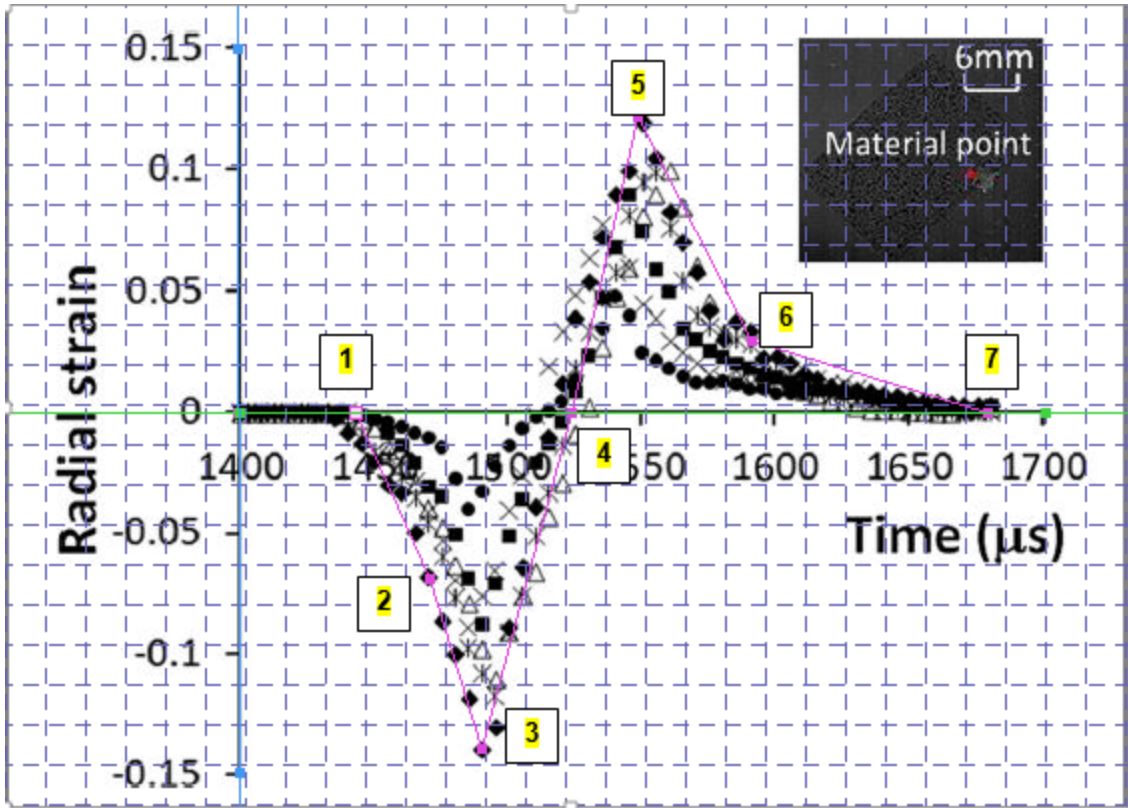


Figure 12 In this figure, the points of reference for table 1 data is marked.

Point #	Time(μ s)	Radstrain (t)	Radial disp(t) (m)	Force (t) (N)	Stress(t) (pa)@ microtubule	T= stress(t)/E
1	43.18	-8.28E-04	-2.07E-09	-3.85926E-15	8438.216561	0.888233
2	70.55	-0.069	-1.73E-07	-3.21605E-13	703184.7134	74.01944
3	89.73	-0.14005	-3.50E-07	-6.52764E-13	1427261.146	150.238
4	123.57	-8.28E-04	-2.07E-09	-3.85926E-15	8438.216561	0.888233
5	148.44	0.121823	3.05E-07	5.67809E-13	-1241508.28	-130.685
6	224.82	0.0339	8.48E-08	1.58006E-13	-345477.707	-36.3661
7	278.41	-8.29E-04	-2.07E-09	-3.86252E-15	8445.350318	0.888984

Table 1 Values of radial strain, radial force, and the radial stress at different points on the radial strain vs time plot.

In previous studies, viscoelastic models were built based on Kelvin model to study the effect of axial force on tau proteins and microtubules in an axon. [16].

Based on this model, when radial strain is applied to the axon because of bubble collapse, the axial stress causes sliding and stretching of tau proteins and its effect on microtubule is studied.

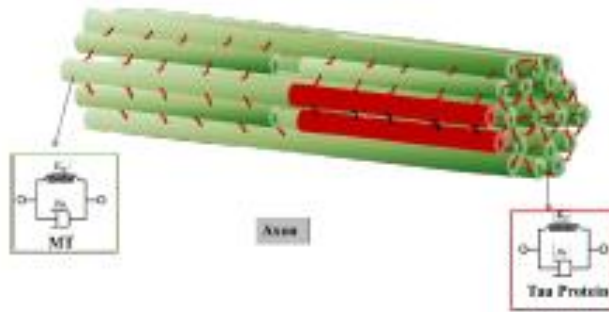


Figure 13 Axon cross section showing tau protein and microtubules.

The mechanical response of axons depends on two dimensionless parameters L/L_c and $\eta\dot{\epsilon}$. Mechanical failure occurs either due to relative sliding of MTs because of stretch of tau proteins or by stretching of the MTs. [10]

From Kelvin viscoelastic model with spring stiffness K in parallel with a dashpot with viscosity μ is used for tau proteins. MTs break at strain rates of $22-44s^{-1}$

Using matlab code given in the appendix, a system of governing equations were used to observe the stretching in microtubules because of the axial stress with time.

CHAPTER 7 CONCLUSIONS AND RESULTS.

The below figures are used to see at what time intervals does the microtubule in the axon fails.

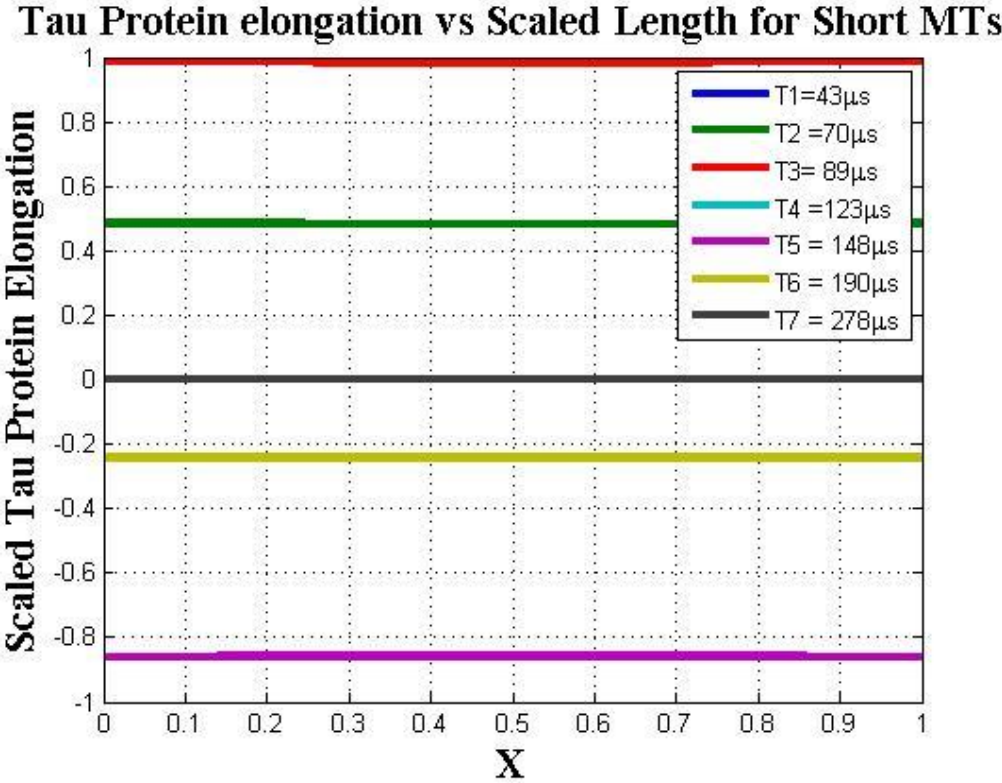


Figure 14 Scaled Tau protein elongation vs Half-length of microtubule.

Maximum MT strain vs Scaled Length for Short MTs

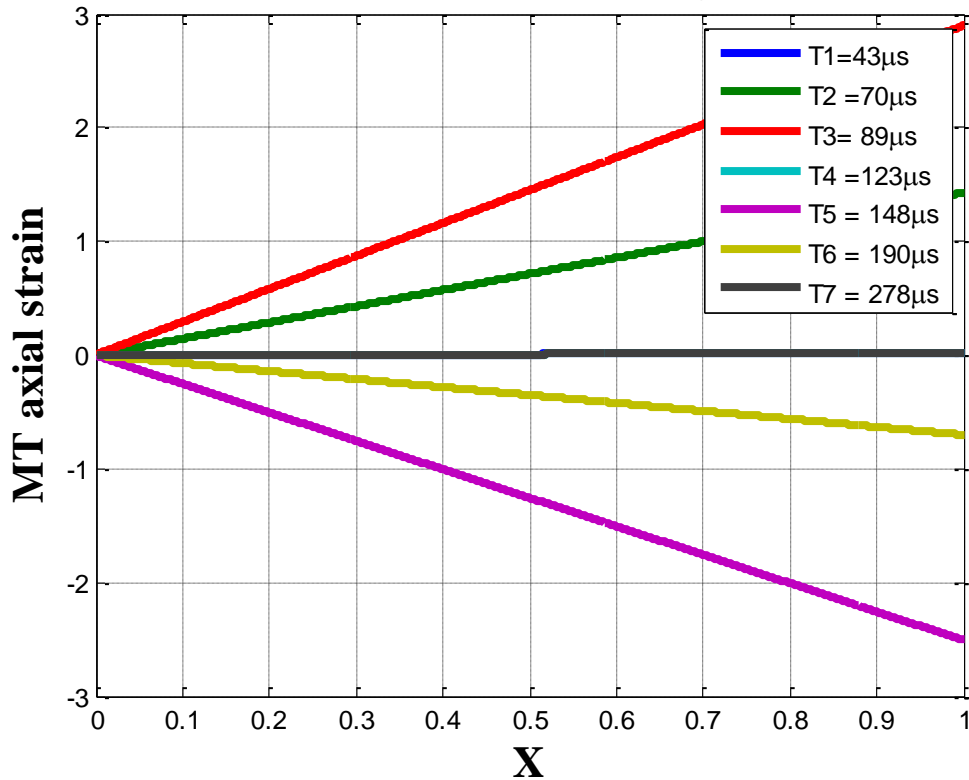


Figure 15 MT axial strain vs half-length of microtubule.

From this we find that after around 40 microseconds of cavitation bubble collapse, the microtubules in axon fail. The DAI is very much present in a brain tissue when cavitation bubbles are formed. The effect of bubble collapse in brain tissue causes more strains leading to DAI than just considering the effect of blasts alone.

Appendix A
Matlab script

```
%MATLAB CODE
```

```
clear all; clc; close all
```

```
t=35e-3;
```

```
L=1e-6;%microm*****change of
```

```
length*****
```

```
T= (63457.03*L/9500);
```

```
Ro=12.5e-9;%nm
```

```
Ri=7e-9;%nm
```

```
Em=1.9e9;%Gpa
```

```
K=0.25e-3;%N/m
```

```
mu=70;
```

```
alpha=6;
```

```
beta=60;%deg
```

```
%dM=20e-9;%nm not used
```

```
dT=60e-9;%nm
```

```
Lc= sqrt((pi*(Ro^2-Ri^2)*dT*(Em+mu/t))/(2*alpha*K*0.5))
```

```
Xint = 0.01;
```

```
format long
```

```

%% 1

ee=0.355*0;

T=-1579.28

x=0:Xint:1;

aa=Lc/(L*sqrt((ee/T)+1));

si=T/(1+((2*aa)*coth(1/(2*aa))));

u11a1=si*(x+(aa*(sinh(x/aa)+(coth(1/(2*aa))*(1-cosh(x/aa))))));

u21a1=(si*(x-(aa*(sinh(x/aa)+(coth(1/(2*aa))*(1-cosh(x/aa))))))+T-si;

du11a1=si*(1+(cosh(x/aa))-(coth(1/(2*aa))*sinh(x/aa)));

%-----%

```

```

%% 2

ee=0.355*(-2.99e-9);

T=-131607

x=0:Xint:1;

aa=Lc/(L*sqrt((ee/T)+1));

si=T/(1+((2*aa)*coth(1/(2*aa))));

u11a2=si*(x+(aa*(sinh(x/aa)+(coth(1/(2*aa))*(1-cosh(x/aa))))));

u21a2=(si*(x-(aa*(sinh(x/aa)+(coth(1/(2*aa))*(1-cosh(x/aa))))))+T-si;

du11a2=si*(1+(cosh(x/aa))-(coth(1/(2*aa))*sinh(x/aa)));

%-----%

```

%%3

ee=0.355*(-2.99e-9);

T=-267124

x=0:Xint:1;

aa=Lc/(L*sqrt((ee/T)+1));

si=T/(1+((2*aa)*coth(1/(2*aa))));

u11a3=si*(x+(aa*(sinh(x/aa)+(coth(1/(2*aa))*(1-cosh(x/aa))))));

u21a3=(si*(x-(aa*(sinh(x/aa)+(coth(1/(2*aa))*(1-cosh(x/aa))))))+T-si;

du11a3=si*(1+(cosh(x/aa))-(coth(1/(2*aa))*sinh(x/aa)));

%-----%

%%4

ee=0.355*(4.46e-9);

T=-1579.28

x=0:Xint:1;

aa=Lc/(L*sqrt((ee/T)+1));

si=T/(1+((2*aa)*coth(1/(2*aa))));

u11a4=si*(x+(aa*(sinh(x/aa)+(coth(1/(2*aa))*(1-cosh(x/aa))))));

u21a4=(si*(x-(aa*(sinh(x/aa)+(coth(1/(2*aa))*(1-cosh(x/aa))))))+T-si;

du11a4=si*(1+(cosh(x/aa))-(coth(1/(2*aa))*sinh(x/aa)));

%-----%

%%5

ee=0.355*4.46e-9;

T=-232358.9

x=0:Xint:1;

aa=Lc/(L*sqrt((ee/T)+1));

si=T/(1+((2*aa)*coth(1/(2*aa))));

u11a5=si*(x+(aa*(sinh(x/aa)+(coth(1/(2*aa))*(1-cosh(x/aa))))));

u21a5=(si*(x-(aa*(sinh(x/aa)+(coth(1/(2*aa))*(1-cosh(x/aa)))))))+T-si;

du11a5=si*(1+(cosh(x/aa))-(coth(1/(2*aa))*sinh(x/aa)));

%-----%

%%6

ee=0.355*4.46e-9;

T=-64659

x=0:Xint:1;

aa=Lc/(L*sqrt((ee/T)+1));

si=T/(1+((2*aa)*coth(1/(2*aa))));

u11a6=si*(x+(aa*(sinh(x/aa)+(coth(1/(2*aa))*(1-cosh(x/aa))))));

u21a6=(si*(x-(aa*(sinh(x/aa)+(coth(1/(2*aa))*(1-cosh(x/aa)))))))+T-si;

du11a6=si*(1+(cosh(x/aa))-(coth(1/(2*aa))*sinh(x/aa)));


```

%-----%
%%7
ee=0.355*2.08e-11;
T=-1580.62
x=0:Xint:1;
aa=Lc/(L*sqrt((ee/T)+1));
si=T/(1+((2*aa)*coth(1/(2*aa))));
u11a7=si*(x+(aa*(sinh(x/aa)+(coth(1/(2*aa))*(1-cosh(x/aa))))));
u21a7=(si*(x-(aa*(sinh(x/aa)+(coth(1/(2*aa))*(1-cosh(x/aa))))))+T-si;
du11a7=si*(1+(cosh(x/aa))-(coth(1/(2*aa))*sinh(x/aa)));
%-----%
figure(1)
plot(x,u21a1-u11a1,x,u21a2-u11a2,x,u21a3-u11a3,x,u21a4-u11a4,x,u21a5-
u11a5,x,u21a6-u11a6,...
x,u21a7-u11a7,'Linewidth',3)
I = legend( '$T1$ = 1443 micro s', '$T2$ =1470 micro s','$T3$ = 1489 micro
s',...
'$T4$ =1523 micro s','$T5$ = 1548 micro s','$T6$ = 1590micro s','$T7$ =
1678micro s');set(I,'interpreter','latex');
title('Tau Protein elongation vs Scaled Length for Short
MTs','FontWeight','bold','FontSize',16,'FontName','Times New Roman');

```

```

xlabel('X','FontWeight','bold','FontSize',16,'FontName','Times New Roman');
ylabel('Tau Protein
Elongation','FontWeight','bold','FontSize',16,'FontName','Times New Roman');
grid on;
%-----%

figure(2)
plot(x,du11a1,x,du11a2,x,du11a3,x,du11a4,x,du11a5,x,du11a6,x,du11a7,'Linewi
dth',3)
I = legend('T1$ = 1443 micro s', 'T2$ =1470 micro s','T3$ = 1489 micro
s',...
'T4$ =1523 micro s','T5$ = 1548 micro s','T6$ = 1590micro s','T7$ =
1678micro s');
set(I,'interpreter','latex');
title('Maximum MT strain vs Scaled Length for Short
MTs','FontWeight','bold','FontSize',16,'FontName','Times New Roman');
xlabel('X','FontWeight','bold','FontSize',16,'FontName','Times New Roman');
ylabel('MT axial strain','FontWeight','bold','FontSize',16,'FontName','Times New
Roman');
grid on;

```

REFERENCES

1. Brookings Institution, Saban Center for Middle East Policy. Iraq index: tracking variables of reconstruction and security in post-Saddam Iraq. April 27, 2010. Available at: www.brookings.edu/iraqindex. Accessed May 2, 2010.
2. Delius M (2002) Twenty years of shock wave research at the institute for surgical research. *Eur Surg Res* 34:30–36.
3. Kato K, Fujimura M, Nakagawa A, Saito A, Ohki T, Takayama K, Tominaga T (2007) Pressure-dependent effect of shock waves on rat brain: Induction of neuronal apoptosis mediated by a caspasedependent pathway. *J Neurosurg* 106:667–676.
4. Rosenfeld JV, McFarlane AC, Bragge P, Armonda RA, Grimes JB, Ling GS (2013) Blast-related traumatic brain injury. *Lancet Neurol* 12:882–893.
5. Y Hong, M. Sarntinoranont¹ & G. Subhash¹ & S. Canchi¹ & M.A. King² (2014) Localized Tissue Surrogate Deformation due to Controlled Single Bubble Cavitation.
6. Brennen CE (1995) Cavitation and bubble dynamics. Oxford University Press, New York.
7. Dissertation (2004.); zur Erlangung des Doktorgrades, der Mathematisch

{Naturwissenschaftlichen FakultÄaten, der Georg {August {UniversitÄat
zu GÄottingen. Referent: Prof. Dr. Werner Lauterborn.

8. Hossein Ahmadzadeh, Douglas H. Smith, and Vivek B. Shenoy, (2015)
Mechanical Effects of Dynamic Binding between Tau Proteins on
Microtubules during Axonal Injury.
9. Hui Ouyang, Eric Nauman and Riyi Shi, 2013; Contribution of
cytoskeletal elements to the axonal mechanical properties.
10. Hossein Ahmadzadeh, Douglas H. Smith, and Vivek B. Shenoy, (March,
2014) Viscoelasticity of Tau Proteins Leads to Strain Rate-Dependent
Breaking of Microtubules during Axonal Stretch Injury: Predictions from
a Mathematical Model.
11. Douglas H. Smith and David F. Meaney, 2000: Axonal Damage in
Traumatic Brain Injury.
12. Min D. Tang-Schomer, Victoria E. Johnson, Peter W. Baas, William
Stewart, Douglas H. Smith, 2011; Partial interruption of axonal transport
due to microtubule breakage accounts for the formation of periodic
varicosities after traumatic axonal injury.
13. Faul, M., Xu, L., Wald, M.M., Coronado, V.G., 2010. Traumatic brain
injury in the United States: emergency department visits, hospitalizations,
and deaths. Centers for Disease Control and Prevention, National Center
for Injury Prevention and Control, Atlanta (GA).

14. Dennerll, T.J., Lamoureux, P., Buxbaum, R.E., Heidemann, S.R., 1989.
The cyto mechanics of axonal elongation and retraction. *J. Cell Biol.* 109,
3073–3083.
15. Gennarelli, T.A., Thibault, L.E., Adams, J.H., Graham, D.I., Thompson,
C.J., Marcincin, R.P., 1982. Diffuse axonal injury and traumatic coma in
the primate. *Ann. Neurol.* 12, 564–574.
16. Jonnalagadda Manikanta, December 2015, TBI induced rate dependent
viscoelastic response of axon: Predictions from a mathematical model.
17. Zink, E.K & Mc. Quillan K.A (2005), *Managing Traumatic Brain Injury,*
Nursing, 36-43.
18. Tang- Schomer, M.D Patel, Smith P.W (2010) Mechanical breaking of
microtubules in axons during dynamic stretch injury underlies delayed
elasticity, microtubule disassembly, and axon degeneration. *The FASEB*
Journal, 1401-1410.
19. Stuhmiller, JH Phillips, Richmond Y.Y (1991), The physics and
mechanisms of primary blast injury. In *conventional warfare: Ballistic,
Blast, and burn injuries* (pp. 241-270), Washington DC.
20. Smith D.H & Meaney , D.F (2000) Axonal damage in traumatic brain
injury. *The neuroscientist,* 483-495.
21. Wright, R.M (2012, January); *A computational model for Traumatic Brain
Injury based on Axonal injury criterion.* Baltimore, MD.

22. Graham DI, Adams JH, Genneralli TA, Mechanisms of non- penetrating head injury. *PRog Clin Biol Res* 1998, 234:159-68.
23. Adams JH, Graham DI, Genneralli TA, Diffuse Axonal injury due to nonmissile head injury in humans: an analysis of 45 cases. *Ann Neurol* 1982;12:557-63.
24. Ahmadzadeh, H. Smith, DH. & Shenoy V.B. (2014). Viscoelasticity of tau proteins leads to strain-rate dependent breaking of microtubules during axonal stretch injury: predictions from a mathematical model. *Biophysical Journal*. 1123-1133.
25. Kevin D. Browne, Xiao- Han Chen, David F. Meany

BIOGRAPHICAL INFORMATION

Divya Bandaru was born and raised in Hyderabad, India. She completed her bachelors in Mechanical engineering from Vasavi College of Engineering, Osmania University. From campus placements she secured a job at QuEST global pvt ltd, Bangalore where she worked with R&D team of Siemens Industrial Turbomachinery in Fingspong, Sweden (Client) as mechanical design engineer. She worked on projects of designing the acoustic packaging components of Industrial gas turbines. While working on the design of Gas Turbines, Divya realized the passion she had for the subject and wanted to pursue higher studies. She came to the US in December 2013 to pursue her Masters in Mechanical Engineering. She joined The University of Texas at Arlington in spring '14. At UTA she worked as graduate teaching assistant for finance and real estate department.

Under the guidance of Dr. Ashfaq Adnan, she started her research for thesis in January 2015. She worked on finding viscoelastic models and viscoelastic stress analysis for different materials like polymer adhesives and on biomaterial such as brain tissues.